Measurement of the atomic Cs[$6^2P_{3/2}(F_e=5)$] hyperfine level effective decay rate near a metallic film with diode laser retrofluorescence spectroscopy

Jean-Marie Gagné and Claude Kondo Assi

Laboratorie d'Optique et de Spectroscopie, Département de Génie Physique, École Polytechnique de Montréal, C.P. 6079, Succ. Centre-Ville, Montréal, Québec H3C 3A7, Canada

Karine Le Bris

Département de Chimie, Université de Montréal, Montréal, Québec H3T 1J4, Canada

Received December 16, 2004; revised manuscript received April 21, 2005; accepted April 23, 2005

Sub-Doppler signals of the hyperfine Cs[$6^2P_{3/2}(F_e)\rightarrow 6^2S_{1/2}(F_g)$] transition lines in a diode laser-induced retrofluorescence spectrum at the interface between glass and Cs vapor are, for the first time to our knowledge, experimentally identified and phenomenologically investigated. We propose a qualitative explanation of the origin of the sub-Doppler hyperfine line, based on kinematic effects of the population of the excited $6^2P_{3/2}(F_e)$ atoms of the laser-pumped velocity classes confined in the near-field region of the interface. The role played by different relaxation processes contributing to the retrofluorescent atomic linewidth has been characterized. The effective decay rate of the atomic hyperfine level $6^2P_{3/2}(F_e=5)$ near a metallic thin film has been measured by using both sub-Doppler retrofluorescence and frequency-modulated selective reflection spectroscopies. For a saturated Cs vapor in a glass cell at a temperature of 130°C, the effective nonradiative relaxation rate of the $6^2P_{3/2}(F_e=5)$ energy hyperfine level due to the coupling with a metallic film is estimated to be $A^{\mathrm{nf}}_{F_e=5\rightarrow F_g=4} \approx 3.10^8\ \mathrm{s}^{-1}$. © 2005 Optical Society of America

OCIS codes: 240.0310, 260.2510, 300.2530, 300.6210.

1. INTRODUCTION

The study of the integrated retrofluorescent spectral signals generated with a diode laser at the interface between a metallic vapor optically thick at resonance and a surface composed of adsorbed atoms, metallic clusters, and atoms chemically bonded to the surface is a promising new way of experimental spectroscopic research for the *in situ* determination of the physical properties of interfaces. The retrofluorescence spectroscopy method is complementary to the methods of selective reflection spectroscopy and evanescent wave spectroscopy.[1,2] In Refs. 3,4 the authors have used a nonradiative and noncollisional mechanism of relaxation of the excited atomic level in the vicinity of a metallic film to interpret the inhibition effect of the spectral retrofluorescent signal observed at the interface between glass and saturated Cs vapor optically thick at resonance. Moreover, these authors mentioned the existence of a sub-Doppler spectral structure located in the spectral region of inhibition of the retrofluorescent signal associated with the 852.2 nm resonant line. The phenomenological model developed[3,4] does not allow, in its present form, the identification and explanation of the origin of this sub-Doppler spectral structure.

In this paper our objective is to present experimental results that corroborate the existence of a spectral substructure in the retrofluorescence signal associated with the resonant 852.2 nm ($6^2P_{3/2}-6^2S_{1/2}$) line at the interface between glass and Cs vapor at a temperature around 130°C. Using frequency-modulated (FM) selective reflection spectroscopy, we show by comparison that this substructure really corresponds to the sub-Doppler hyperfine structure of the atomic $6^2P_{3/2}\leftarrow 6^2S_{1/2}$ absorption line. We have measured and analyzed the profiles of the cycling ($F_e=5\rightarrow F_g=4$) hyperfine spectral line of the retrofluorescence and FM selective reflection spectra. Starting with the spectral properties of this sub-Doppler hyperfine line, we propose and carry out an experimental method allowing the *in situ* measurement of the effective decay rate of the population of atoms, excited in the atomic $6^2P_{3/2}(F_e=5)$ hyperfine level, which is located near a metallic film.

By using these measurements, and the physical concepts of the methods of selective reflection spectroscopy[5,6] and of retrofluorescence spectroscopy,[3] we estimate the effective decay rate due only to the nonradiative relaxation process of the excited atomic level in the vicinity of a metallic film. The value of the effective nonradiative decay rate due to the coupling of the excited atom with the metallic surface, $A^{\mathrm{nf}}_{F_e=5\rightarrow F_g=4}$, obtained by using this new

method and based on the retrofluoresecence sub-Doppler effect, is compared with the values measured by Le Bris *et al.*[3] and Gagné *et al.*[4]

2. EXPERIMENTAL SETUP

The diode laser-induced retrofluorescence spectroscopy technique reported here is the same as the one described in Ref. 3. The experimental setup is illustrated in Fig. 1. The Cs cell is embedded in an aluminum block and heated to a programmed temperature (between 90° and 180°C), controlled by a Mirak thermometer (Model HP72935). A diode laser from Environmental Optical Sensors, Inc. (Model LCU 2001), with a bandwidth below 10 MHz, is used to excite the Cs atomic vapor around the 852 nm resonance line. We limited ourselves to weak laser powers (between 20 and 570 μW for a beam area of $\sim$0.014 cm^2) to avoid nonlinear effects. The calibration was carried out with a Fabry–Perot interferometer by directing a fraction of the exciting laser beam to it. The main laser beam is directed to the cylindrical Cs cell along the cell axis at an angle of incidence of $\sim$2° with respect to the normal of the entrance window surface. The fluorescence emitted backward at an angle of $\sim$16° with respect to the normal of the surface was captured by a 0.5 m focal-length Jarell Ash spectrometer (Model 5) equipped with a photomultiplier. The fluorescence signals were amplified by a picoammeter (Keithley Instruments) and were then digitized and recorded by a computer. FM selective reflection spectroscopy signals were simultaneously collected by a Si photodiode. For studies at high resolution related to the hyperfine structures of the Cs ground state covering a bandwidth of 20 GHz, we used a piezoelectric device having a resolution of a few megahertz to ensure the spectral stepping of the laser sweep.

3. RESULTS

Figure 2(a) shows the integrated retrofluorescence spectrum and Fig. 2(b) shows the FM selective reflection spectrum generated at the glass–Cs vapor interface at a temperature $\sim$130°C and a laser power $\sim$50 μW when the diode laser is tuned over the 852.2 nm ($6^2S_{1/2} \rightarrow 6^2P_{3/2}$) atomic transition line for a bandwidth laser sweeping of 20 GHz. As mentioned in Ref. 3 and as specified in Fig. 2, the simultaneous measurement of the FM selective reflection and retrofluorescence spectra shows that the deep dips in the retrofluorescence spectrum correspond, as a first approximation, to the centers of the two transitions lines $6^2S_{1/2}(F_g=3) \rightarrow 6^2P_{3/2}$ and $6^2S_{1/2}(F_g=4) \rightarrow 6^2P_{3/2}$ associated with the hyperfine structure of the ground state $6^2S_{1/2}$, energetically separated from each other by a gap of 9.2 GHz. For different cell temperatures ($<$150°C), we observe a weak spectral substructure signal in the deep dips of the retrofluorescence spectrum as previously mentioned.[3]

For the identification and a detailed analysis of the substructure, we choose as an example the spectral band corresponding to the deep dip of the spectral line associated with the $6^2S_{1/2}(F_g=4) \rightarrow 6^2P_{3/2}$ transition. The analysis performed on this spectral line can easily be extended

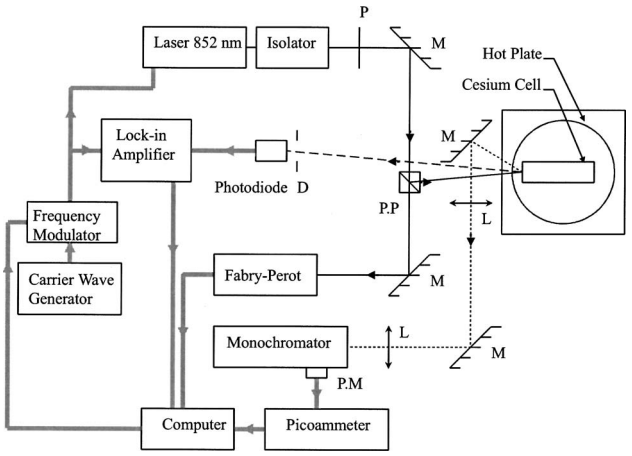

Fig. 1. Schematic of the experimental setup. P, polarization rotator; L, lens; M, mirror; P.P., polarizing prism; P.M., photomultiplier; D, spatial filter.

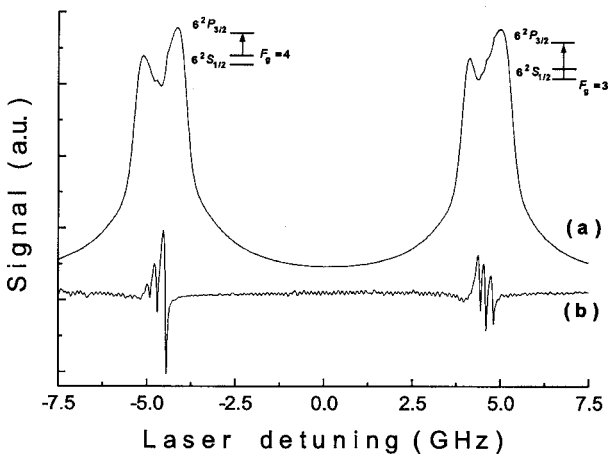

Fig. 2. (a) Integrated retrofluorescence spectrum at a 852.2 nm wavelength as a function of the laser detuning for a cell temperature $\sim$130°C and laser power $\sim$50 μW. (b) Simultaneous recording of the FM selective reflection spectrum.

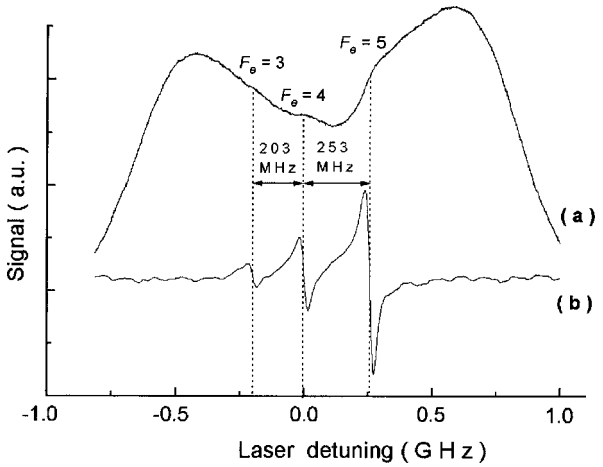

Fig. 3. (a) Enlarged plot of the integrated 852.2 nm resonant retrofluorescence and (b) the FM selective reflection spectra as a function of laser detuning from the resonance center for the $[6^2S_{1/2}(F_g=4) \rightarrow 6^2P_{3/2}(F_e=3,4,5)]$ transition obtained at a temperature $\sim$130°C and laser power $\sim$50 μW.

to the $6^2S_{1/2}(F_g=3)\rightarrow 6^2P_{3/2}$ line. To this end, Fig. 3(a) displays an enlarged plot of the integrated retrofluorescence and Fig. 3(b) shows the FM selective reflection spectra in the inhibition spectral region for the optical $[6^2S_{1/2}(F_g=4)\rightarrow 6^2P_{3/2}]$ pumping transition, obtained at a temperature ~130 °C. Since the FM selective reflection spectra of Cs vapor are well known,[5] we use them [Fig. 3(b)] as reference frequency scaling spectra and for comparison to identify the substructure observed in the retrofluorescence signal. The high-resolution analysis (with a data recording frequency stepping of the order of megahertz) reveals, as a first approximation, that the peaks of the substructure coincide in frequency position with the three reference lines of the sub-Doppler signal obtained in selective reflection spectroscopy. Accordingly, this retrofluorescent substructure reflects the signature of the hyperfine structure of the excited $6^2P_{3/2}(F_e=3,4,5)$ level when the pumping laser is tuned over the resonant $6^2S_{1/2}(F_g=4)\rightarrow 6^2P_{3/2}$ transition. As in selective reflection spectroscopy, no Doppler cross resonances were observed in the retrofluorescence spectra. Similar results were obtained when we analyzed the $6^2S_{1/2}(F_g=3)\rightarrow 6^2P_{3/2}$ line, i.e., the substructure is attributed to the hyperfine structure of the excited $6^2P_{3/2}(F_e=2,3,4)$ levels.

4. HYPERFINE SPECTRAL DATA ANALYSIS AND DISCUSSION

Using the spectral properties of the sub-Doppler cycling hyperfine $[6^2S_{1/2}(F_g=4)\rightarrow 6^2P_{3/2}(F_e=5)]$ line, which is the strongest of the structure, we propose and carry out an experimental method allowing the measurement of the effective decay rate of the atomic $6^2P_{3/2}(F_e=5)$ hyperfine level in the presence of a near-metallic thin film. To this end, one must extract and analyze this hyperfine spectral line. In Subsections 4.A–4.C we present an extraction of the sub-Doppler hyperfine line profile from the integrated retrofluorescence signal, a phenomenological description of the origin of the sub-Doppler signal, and an experimental characterization of the $[6^2P_{3/2}(F_e=5)\rightarrow 6^2S_{1/2}(F_g=4)]$ transition linewidth.

A. Experimental Sub-Doppler Hyperfine Line Shape

In this subsection we propose to extract the experimental hyperfine line profile, which is added to the integrated retrofluorescence spectral signal $S^T(\nu_L)$ that has been previously analyzed.[3] $S^T(\nu_L)$ has been associated with the $6^2P_{3/2}$ excited atoms population, completely redistributed. $S^T(\nu_L)$ has the following form[3]:

$$S^T(\nu_L) \propto \alpha_T(\nu_L)\exp[-\bar{\tau}_T^f(\nu_L)] \times \int_{\Delta\nu} \frac{\alpha_T(\nu)}{\alpha_T(\nu_L)+\alpha_T(\nu)}\exp[-\bar{\tau}_T^f(\nu)]\mathrm{d}\nu, \quad (1a)$$

where $\alpha_T(\nu_L)$ is the normalized profile of the effective atomic absorption coefficient of the $F_e=3,4,5$ hyperfine lines at the laser frequency ν_L; $\alpha_T(\nu)$ is the normalized profile of the effective atomic emission at frequency ν in the vapor region far away from the cell entrance window where surface effects on the excited atoms are practically negligible; $\bar{\tau}_T^f(\nu_L)$ is the effective spectral optical thickness at laser frequency ν_L of the so-called stop-band filter[3] for the atomic hyperfine transition between the ground hyperfine level $F_g=4$ and the overall excited levels $F_e=3,4,5$; and $\bar{\tau}_T^f(\nu)$ is the effective spectral optical thickness of the stop-band filter at frequency ν.

We can extract the experimental hyperfine signal $s^n{}_{\exp}(\nu_L)$ by subtracting $S^T(\nu_L)$, given by Eq. (1a), from the total experiment signal $S^{\mathrm{ob}}(\nu_L)$. However, as a first approximation, to evaluate the essential spectral characteristics of the hyperfine $F_e=5\rightarrow F_g=4$ line, we use a direct and simple method. To this end, we approximate $S^T(\nu_L)$ by using an affine function $a(\nu_L-\nu_0)+b$ in the ~100 MHz spectral band centered on the $F_e=5\rightarrow F_g=4$ line, where a and b are constants determined experimentally. This linear approximation is illustrated in Fig. 4(a) where the dashed curve represents the approached function of $S^T(\nu_L)$. We have

$$s^n{}_{\exp}(\nu_L) = S^{\mathrm{ob}}(\nu_L) - S^T(\nu_L) \approx S^{\mathrm{ob}}(\nu_L) - [a(\nu_L-\nu_0)+b]. \quad (1b)$$

We scaled the frequency axis by using the well-known gap between the two reference hyperfine lines $F_e=5\rightarrow F_g=4$ and $F_e=4\rightarrow F_g=4$ (value of 253 MHz), whose positions

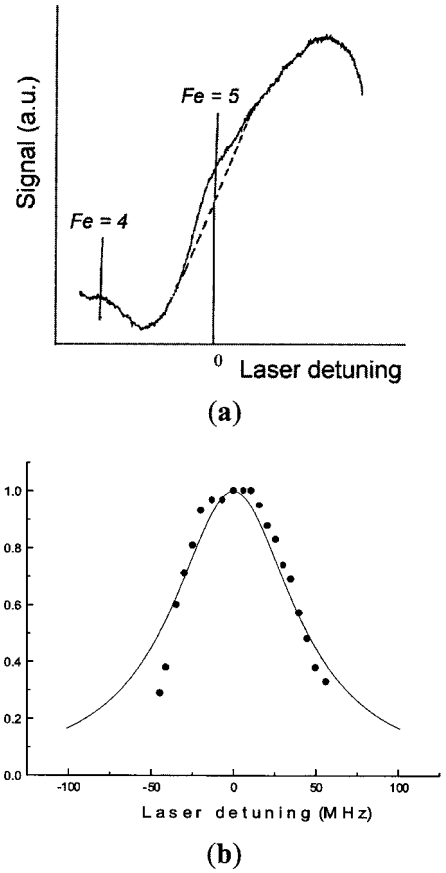

Fig. 4. (a) Extraction of the hyperfine $[6^2P_{3/2}(F_e=5)\rightarrow 6^2S_{1/2}(F_g=4)]$ transition signal profile. The dashed curve represents the approached function of $S^T(\nu_L)$; the vertical line ($F_e=5$) indicates the center of the hyperfine line. (b) Distribution of the points in the ~100 MHz width spectral band around the ($F_e=5\rightarrow F_g=4$) transition line center, obtained after subtraction of $S^T(\nu_L)$ from the experimental data. The solid curve is a Lorentzian fit of experimental points.

were determined by FM selective reflection spectroscopy. The frequency sweep is linear in the spectral band of interest. Each point of the hyperfine signal profile is obtained by subtracting the value of $S^T(\nu_L)$ from the measured signal $S^{ob}(\nu_L)$ for frequency interval samples ~5–10 MHz. The spectral distribution of points obtained by this method in the central area (~100 MHz spectral band centered on the line) and normalized to unity at the maximum is shown in Fig. 4(b). It is well known that the resonance collisional broadening at the center of the line and in the wings differs in magnitude and mechanism.[5] The x axis is the laser frequency detuning $\Delta\nu_L$ from the hyperfine $F_e=5\rightarrow F_g=4$ line center ν_0.

A fit of the normalized profile of the data [Fig. 4(b)] corresponding to the spectral band (~100 MHz) centered on the cycling $F_e=5\rightarrow F_g=4$ hyperfine transition line is obtained by using a Lorentzian distribution function with a 90 MHz full width at half-maximum. We note an agreement of the Lorentzian fit with the experimental data of the line profile. The full width at half-maximum of the spectral profile obtained is estimated to be $\gamma_{RF}\sim 90$ MHz. Note that γ_{RF} is greater than the natural linewidth γ_n ~5.3 MHz, but is smaller than the Doppler width γ_D ~0.4 GHz.

B. Origin of the Sub-Doppler Signal

In this subsection we propose a phenomenological qualitative explanation of the origin of the sub-Doppler hyperfine line and we justify the Lorentzian-type profile of the experimental spectral line. For that, we consider the thermalization processes and the kinematic properties of a velocity class of excited atoms in a thin vapor layer near the cell entrance window. The sub-Doppler signal is associated with the kinematic properties of the population of a velocity class, which is confined in a thin vapor layer in contact with a metallic film. In Subsections 4.B.1–4.B.3, respectively, we briefly recall the geometric and physical modeling of the glass–Cs vapor interface, the thermalization processes in a pure Cs vapor and the kinematic properties of the laser-pumped velocity classes of the excited $6^2P_{3/2}(F_e)$ atoms, and then we explain the origin of the sub-Doppler signal.

1. Geometric and Physical Modeling of the Glass–Cs Vapor Interface

Figure 5 shows a schematic representation of the geometric and physical properties of the interface between the glass cell window and the Cs vapor. Because of its exposure to the saturated Cs vapor, the internal surface of the glass cell is covered by a thin metallic Cs film, probably composed of clusters, adsorbed atoms, atoms chemically bonded to the surface, and atoms diffused into the glass (region a). The thin vapor layer (region b) in the vicinity of the cell surface is designated as the optical near-field region of the interface, which has a thickness of $\bar{x}_f<\lambda$. Region c, far away from the surface, designated as the far-field region, is a semi-infinite vapor next to the near-field region. In the present work we complement the simple model[3] by taking account of the signal generated in the near-field region. This sub-Doppler signal, having its origin in the near-field region, is designated by $s^n(\nu_L)$ in Fig. 5.

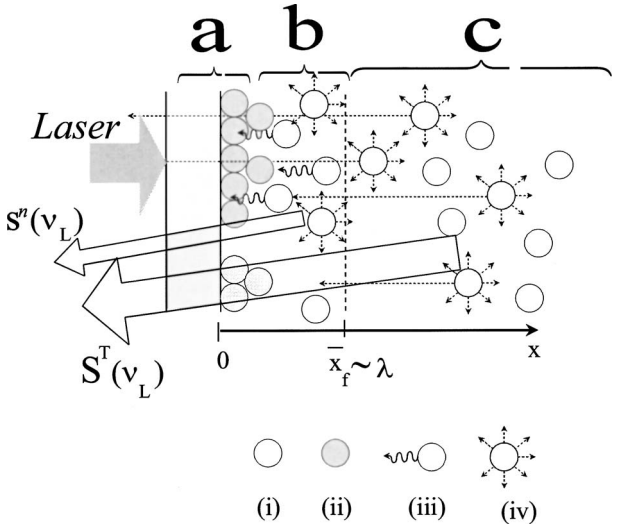

Fig. 5. Physical and geometric description of the characteristic regions of the glass cell window and Cs vapor interface: a, thin Cs metallic layer on the glass surface; b, proximity region of the surface ($\bar{x}_f\approx\lambda$) called the near-field region of the interface; c, the far-field region of the interface. $S^T(\nu_L)$ designates the integrated retrofluorescence signal from the far-field region of the interface. $s^n(\nu_L)$ designates the integrated retrofluorescence sub-Doppler hyperfine signal originating from the near-field region. The objects labeled (i)–(iv) represent a Cs atom in the ground level, an atom adsorbed on the surface or on a Cs cluster, excited Cs atom undergoing a nonradiative relaxation, radiating (or fluorescent) atom, respectively.

2. Thermalization Processes in a Pure Cs Vapor

According to Huennekens *et al.*,[7] in a pure Cs vapor, photon trapping processes and resonance exchange collisions can lead to substantial thermalization of the excited atom velocity distribution. In our case, in the vapor region far from the cell entrance window, the thermalization process by radiation trapping is more important than that of resonance exchange collisions. The authors of Ref. 7 have noted that, in the case of a vapor layer confined in a thin cell, one can expect that the thermalization due to radiation trapping will be reduced to the point where the resonance collisions can be directly studied. On the basis of their work, it is reasonable to consider that a thin vapor layer of thickness $\bar{x}_f<\lambda$ (λ is the wavelength of the transition) at the interface, that we call the near-field region, can be studied by using the hypothesis of partial thermalization of the population of the excited atoms of a velocity class in the vicinity of the cell entrance window. We take the escape factor of the retrofluorescent photon $[6^2P_{3/2}(F_e=5)\rightarrow 6^2S_{1/2}(F_g=4)]$ emitted from the near-field region close to one. Considering the results of Huennekens *et al.*[7] and considering the fact that trapping effects are negligible in the near-field region, we can assume that a fraction of the population of a velocity class is not completely thermalized in the near-field region of the glass–Cs vapor interface, contrary to the case of the far-field region where trapping effects are important and where the redistribution of the population of the excited $6^2P_{3/2}$ atoms is complete.

As the spectral line considered here has a sub-Doppler spectral width and a Lorentzian-type profile, it is reasonable to associate the origin of the sub-Doppler signal with

the population of a velocity class of atoms of the ground $6^2S_{1/2}(F_g=4)$ level, located in the optical near-field region, which is pumped to the excited $6^2P_{3/2}(F_e=5)$ level by the diode laser. On the velocity axis V_x in the laser beam direction, a certain velocity interval ΔV_x is associated with the spectral width of the $6^2S_{1/2}(F_g=4)\rightarrow 6^2P_{3/2}(F_e=5)$ absorption line.[8] We can write $\Delta V_x=\lambda\gamma$, where γ is the spectral broadening of the transition for a homogeneous broadening related to the different competing relaxation processes of the nonthermalized atoms in the exited state. The atoms in the ground $6^2S_{1/2}(F_g=4)$ level, lying in this velocity interval, that are pumped to the excited $6^2P_{3/2}(F_e=5)$ level constitute the population of the velocity class interacting effectively with the laser. ΔV_x is the width of the velocity class population distribution. The mean velocity $\langle V_x\rangle$ (along the laser propagation direction) of this velocity class at laser frequency ν_L is $\langle V_x\rangle=\lambda(\nu_L-\nu_0)$. Because of the Maxwell–Boltzmann (MB) velocity distribution of the population in the ground state, the distribution of the population of the laser-pumped velocity class is modulated by this MB distribution. Thus the effective distribution of population $D(V_x,\langle V_x\rangle,\Delta V_x)$ of $6^2P_{3/2}(F_e=5)$ atoms of a velocity class, along with the velocity component in the laser propagation direction, normalized to one at the maximum is given by[9]

$$D(V_x,\langle V_x\rangle,\Delta V_x)\propto\frac{1}{[2(\langle V_x\rangle-V_x)/\Delta V_x]^2+1}\exp[-(V_x/V_0)^2], \tag{2}$$

where V_0 is the most probable speed of the MB distribution [$V_0=(2kT/m_{\mathrm{Cs}})^{1/2}$, here k is the Boltzmann constant, T is the vapor temperature, and m_{Cs} is the Cs atom mass].

Considering relation (2), we can outline three kinematic properties of the excited population of a velocity class when $\langle V_x\rangle\geqslant 0$. Note that for $\langle V_x\rangle=0$, the velocity class is composed of two groups of atoms moving in opposite directions $\pm V_x$. When $\langle V_x\rangle\gg 0$, all the atoms of the velocity class move in the same direction as the mean velocity $\langle V_x\rangle$ of the velocity class. In the intermediate case, we have two groups of atoms, with different population numbers, moving in opposite directions.

3. Origin of the Signal and Profile of the Spectral Line

It is reasonable to assume that the atoms of a velocity class, moving away in free flight from their origin in the near-field region before photon emission, do not contribute significantly to the sub-Doppler hyperfine signal generated at the interface. Indeed, the excited atoms colliding with the cell wall do not contribute to the retrofluorescent signal.[10] We also consider that the excited atoms that enter the far-field region do not participate significantly with the sub-Doppler signal because they are either thermalized or the photons emitted in this region are trapped and thermalized.[7] Only the excited $6^2P_{3/2}(F_e)$ atoms of the laser-pumped velocity class having a larger residence time in the thin vapor layer close to the cell entrance window compared to the radiative lifetime (spontaneous emission) may contribute significantly to the sub-Doppler hyperfine signal. It would be interesting to address the possible analogy with the physics of sub-Doppler spectroscopy in a thin film of resonant vapor.[11] There is only a fraction of the initial population of a velocity class that satisfies this residence time constraint in the near-field region. In the velocity space, this fraction of atomic population contributing to the sub-Doppler hyperfine signal is confined in a velocity interval δV_x, centered at the one-dimensional MB velocity distribution of the atoms in the ground $6^2S_{1/2}(F_g=4)$ level, i.e., with a velocity $V_x\approx 0$. In other words, we consider that a fraction of the population of the excited atoms of the velocity class in the near-field region behave practically like a two-dimensional gas normal to the laser beam. The sub-Doppler effect observed is attributed to the fact that the velocity interval δV_x, centered on $V_x=0$, is independent of the mean velocity $\langle V_x\rangle$, as we will explain in the following. As the near-field region (of thickness $\bar{x}_f$) is optically thin at resonance, the atomic population of the velocity class in the interval δV_x is uniform along the x spatial coordinate in the near-field region. The velocity interval δV_x is related to the geometric thickness $\bar{x}_f$ of the vapor layer and the radiative lifetime $\tau_{F_e=5\rightarrow F_g=4}$ of the transition. We consider that δV_x satisfies the following constraint:

$$\delta V_x<\delta V_x^{\max}, \tag{3a}$$

where

$$\delta V_x^{\max}=\bar{x}_f/\tau_{F_e=5\rightarrow F_g=4}=\bar{x}_f g_{F_e=5,F_g=4}A_{J_eJ_g}, \tag{3b}$$

where $g_{F_e=5,F_g=4}=1/2.908$ is the statistical weight of the hyperfine $[6^2P_{3/2}(F_e=5)\rightarrow 6^2S_{1/2}(F_g=4)]$ transition and $A_{J_eJ_g}=3.3.10^7\ \mathrm{s}^{-1}$ is the spontaneous emission rate of the $6^2P_{3/2}$ level. Considering that the escape factor of the photon emitted backward from the near-field region is close to one, then we can write that the optical thickness of this region at resonance ($\nu_L=\nu_0$) is smaller than one:

$$\bar{x}_f n_{F_g=4}\sigma_{F_g=4\rightarrow F_e=5}(\nu_L\approx\nu_0)<1, \tag{4}$$

where $n_{F_g=4}$ is the effective density of hyperfine ground level F_g and $\sigma_{F_g=4\rightarrow F_e=5}(\nu_L\approx\nu_0)$ is the effective cross section for atoms in the near-field region at resonance $\nu_L\approx\nu_0$. The analytic form of $\sigma_{F_g\rightarrow F_e}$ in the presence of a metallic film has been studied by Le Bris *et al.*[3] By using Eqs. (3a), (3b), and (4), we have

$$\delta V_x^{\max}=g_{F_e=5,F_g=4}A_{J_eJ_g}/n_{F_g=4}\sigma_{F_g=4\rightarrow F_e=5}(\nu_L\approx\nu_0). \tag{5}$$

Considering that $\gamma_{\mathrm{RF}}\ll\gamma_{\mathrm{D}}$, we derive the following relation[12]:

$$\sigma_{F_g=4\rightarrow F_e=5}(\nu_L\approx\nu_0)\approx\frac{\lambda^2}{8\pi}\frac{2J_e+1}{2J_g+1}g_{F_e=5,F_g=4}A_{J_eJ_g}\times(1+\epsilon_{F_e=5,F_g=4})\left(\frac{4\ln 2}{\pi}\right)^{1/2}\frac{1}{\gamma_{\mathrm{D}}}, \tag{6a}$$

where

$$\epsilon_{F_e=5,F_g=4} = \frac{A^f_{F_e=5,F_g=4}}{g_{F_e=5,F_g=4} A_{J_e=3/2,J_g=1/2}}, \tag{6b}$$

and $A^f_{F_e=5,F_g=4}$ is the total effective nonradiative decay rate of the excited atom in the near-field region. Putting together Eqs. (5), (6a), and (6b), we have

$$\delta V_x^{\max} \approx \frac{8\pi}{0.93\lambda^2} \frac{2J_g+1}{2J_e+1} \frac{\gamma_D}{(1+\epsilon_{F_e=5,F_g=4})} \frac{1}{n_{F_g=4}}. \tag{7}$$

In this case we are concerned with $J_g=1/2$, $J_e=3/2$, and $n_{F_g=4}=9n/16$ where n is the vapor density $\sim 8.10^{19}$ atoms/m^3 at a temperature of 130°C. Using these values and approximation (7), we have

$$\delta V_x^{\max}(\text{m s}^{-1}) \approx 165(1+\epsilon_{F_e=5,F_g=4})^{-1}. \tag{8}$$

From approximation (8), note that the velocity domain $\delta V_x^{\max}$ is related to the parameter characterizing the effective nonradiative decay rate of the excited atoms in the near-field region.

To illustrate the origin of the sub-Doppler retrofluorescence signal in the velocity space, we use a schematic representation. Figure 6 represents the normalized distribution along the velocity component in the laser beam direction at a spatial coordinate x in the near-field region of the atomic population distribution brought up to the $6^2P_{3/2}(F_e=5)$ excited level by the laser at frequency ν_L. The curve G corresponds to the one-dimensional MB velocity distribution of the population of thermalized atoms at the ground $6^2S_{1/2}(F_g=4)$ level. The curves c_1, c_2, and c_3 represent the effective stationary distributions along the velocity component V_x for different velocity classes of the

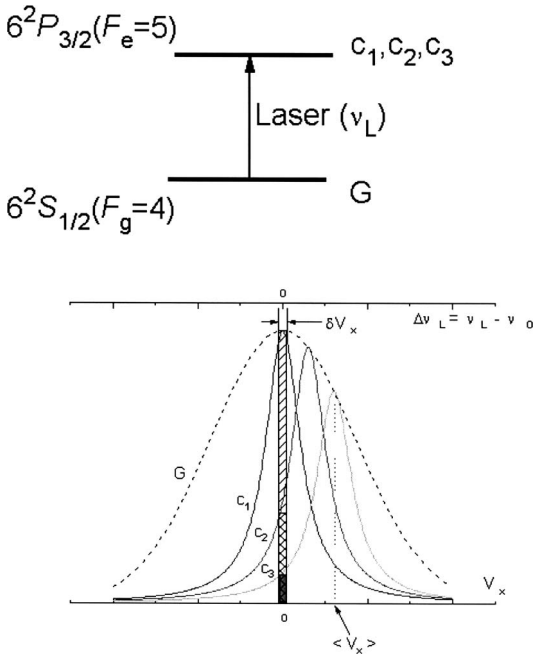

Fig. 6. Illustration of the velocity population distribution of the thermalized $6^2S_{1/2}(F_g=4)$ ground level (G) and the nonthermalized $6^2P_{3/2}(F_e=5)$ excited level population (c_1,c_2,c_3) pumped by a quasi-monochromatic diode laser at frequency ν_L in the near-field region of the cell window and Cs vapor interface. For more details, see the text.

population of excited atoms nonthermalized at the $6^2P_{3/2}(F_e=5)$ level. For a velocity class c_i, corresponding to the laser frequency $(\nu_L)_i$, we have $\langle V_x\rangle_i = \lambda[(\nu_L)_i - \nu_0]$. At laser frequency zero detuning from the resonance line center ν_0, we have $\langle V_x\rangle = 0$. The δV_x width striped slice, centered on $V_x=0$, is proportional to the effective population of radiating atoms in the near-field region that contribute to generate the sub-Doppler hyperfine radiation. Thus we introduce a probability density per unit velocity, $\Pi(V_x, \delta V_x)$, in which an excited atom of velocity V_x in a velocity class contributes effectively to the sub-Doppler retrofluorescent signal. It is reasonable to take

$$\Pi(V_x, \delta V_x) = 1, \quad \text{for } -\delta V_x/2 \leqslant V_x \leqslant +\delta V_x/2$$
$$= 0, \quad \text{elsewhere.} \tag{9}$$

δV_x is the width of the $\Pi(V_x, \delta V_x)$ function centered on $V_x=0$.

On the basis of the preceding paragraph, for a given value of v_L (or $\langle V_x\rangle$), the theoretical integrated retrofluorescence sub-Doppler hyperfine signal $s^n(\langle V_x\rangle)$ originating from the near-field region of the interface is given by

$$s^n(\langle V_x\rangle) \propto \int_{-\infty}^{+\infty} \Pi(V_x, \delta V_x) D(V_x, \langle V_x\rangle, \Delta V_x) \mathrm{d}V_x$$
$$= \Pi(V_x, \delta V_x)^* D(V_x, \langle V_x\rangle, \Delta V_x), \tag{10}$$

where the symbol * denotes the convolution operation. It will be shown in Subsection 4.C that we have

$$\delta V_x^{\max} \ll \Delta V_x, \quad \text{or } 165(1+\epsilon_{F_e=5,F_g=4})^{-1} \ll \Delta V_x; \tag{11}$$

and knowing that the intervals ΔV_x and $\delta V_x^{\max}$ remain practically unchanged for all velocity classes c_i, it is important to emphasize that the normalized theoretical integrated retrofluorescent spectral signal $s^n(\langle V_x\rangle)$, corresponding to the population confined in the velocity interval $\delta V_x^{\max}$ in the near-field region, is proportional to

$$s^n(\langle V_x\rangle) \propto \frac{1}{(2\langle V_x\rangle/\Delta V_x)^2 + 1}. \tag{12}$$

The theoretical signal reproduces a Lorentzian profile with a width ΔV_x corresponding to the velocity class and where $\langle V_x\rangle$ is the experimental variable. The theoretical sub-Doppler signal is maximum when the mean velocity $\langle V_x\rangle$ coincides with the center of the one-dimensional velocity distribution of the ground level. The signal gradually decreases with the laser frequency detuning v_L from the Bohr frequency v_0 of the transition. By writing $\Delta V_x = \lambda\gamma$, $\langle V_x\rangle = \lambda(v_L - v_0)$, and substituting them into relation (12), in the frequency domain one arrives at

$$s^n(v_L) \propto \frac{1}{[2(v_L - v_0)/\gamma]^2 + 1}. \tag{13}$$

As a conclusion to the theoretical model, let us note that the sub-Doppler signal is a homogeneous profile (Lorentzian) and that γ is related to the lifetime of the excited state (or to the total effective decay rate of the excited atoms in the near-field region). We can link this theoretical result to the experimental data of the sub-Doppler hyperfine shape.

The experimental hyperfine sub-Doppler signal profile given in Fig. 4 is reasonably fitted by relation (13) when γ is identified with the experimental linewidth γ_{RF} estimated to be 90 MHz. Thus γ_{RF} is a spectral width, which is characteristic of the atomic excited level $6^2P_{3/2}(F_e=5)$ in the near-field region. Now we need to characterize the spectral width γ_{RF} to evaluate the value of the effective nonradiative decay rate reflecting the coupling of the excited atom with the metallic film, as shown in Fig. 5.

C. Characterization of the Linewidth of the Hyperfine $[6^2P_{3/2}(F_e=5)\rightarrow 6^2S_{1/2}(F_g=4)]$ Signal

To characterize contributions of different relaxation processes contributing to the experimental retrofluorescent atomic line width γ_{RF}, it is necessary to model the evolution of the population of the excited $6^2P_{3/2}(F_e=5)$ level confined in the thin vapor layer near the cell window.

Because the atomic transition of interest can be treated as cycling, we consider the near-field region as a vapor composed of two-level atoms. When the near-field region is irradiated by a quasi-monochromatic laser beam, the vapor behaves like a mixture of Cs atoms in the ground $6^2S_{1/2}(F_g=4)$ level, nonthermalized excited $6^2P_{3/2}(F_e=5)$ atoms and atoms in a coherent state or pure state in the presence of a metallic film. The sub-Doppler retrofluorescence spectroscopic method permits an *in situ* characterization of the nonthermalized excited atoms of a velocity class in the $6^2P_{3/2}(F_e=5)$ level between the cell wall covered by a metallic film and a semi-infinite far-field region.

We consider that the cycling transition line undergoes a homogeneous broadening related to the different competing relaxation processes of the nonthermalized atoms in the $6^2P_{3/2}(F_e=5)$ level. In our elementary analysis we retain three dominant causes generating the relaxation of the excited level: the spontaneous emission process, the process of nonradiative transition of the atomic dipole (atom in the energy hyperfine level) due to the presence of the metallic film, and the resonant elastic collisions processes. Assuming that the relaxation probability is the same for all the excited atoms confined in the near-field region, and taking into account the competing relaxation processes of the $6^2P_{3/2}(F_e=5)$ level, we sum up the corresponding spectral broadening and obtain the following relation:

$$\gamma_{RF} \approx \gamma_n + \gamma_{coll} + \gamma_{nr}, \tag{14}$$

where γ_{coll} is the resonance collisional broadening of the hyperfine line, and γ_{nr} is an additional broadening induced by the nonradiative energy-transfer phenomena of the excited atoms near the cell window surface.[13,14] To evaluate γ_{nr}, we use the FM selective reflection spectroscopy technique.

According to Akul'shin *et al.*[5] and Vuletic *et al.*,[6] for the FM selective reflection for the hyperfine line, the following relation holds:

$$\gamma_{RS} = \gamma_n + \gamma_{coll}, \tag{15}$$

where γ_{RS} is the width of a hyperfine structure spectral line in selective reflection (γ_{RS} is equal to the interval between the extrema on the experimental curve). By using Eqs. (14) and (15), we have

$$\gamma_{nr} \approx \gamma_{RF} - \gamma_{RS}. \tag{16}$$

Considering the ($F_g=4$-$F_e=5$) line of the selective reflection spectra [Fig. 3(b)], we measure the linewidth $\gamma_{RS} \approx 41$ MHz. This value is in agreement with that measured by Akul'shin *et al.*[5] Using the preceding experimental values, we deduce the spectral width associated with the nonradiative relaxation produced by the coupling of the excited atoms in the near-field region with the metallic film:

$$\gamma_{nr} \approx (\gamma_{RF})_{measured} - (\gamma_{RS})_{measured} \approx 90 - 41 = 49 \text{ MHz}. \tag{17}$$

Note that $\gamma_{nr} \approx \gamma_{RS}$. We have $A^{nf}_{F_e=5,F_g=4} = 2\pi\gamma_{nr} \approx 3.10^8 \text{ s}^{-1}$. Using Eq. (15) and the value $\gamma_n \sim 5.3$ MHz, we obtain $\gamma_{coll} = 35.7$ MHz. The value of the nonradiative decay rate associated with the collisions is $A^{coll}_{F_e=5,F_g=4} = 2\pi\gamma_{coll} \approx 2.24 \times 10^8 \text{ s}^{-1}$. Using both preceding nonradiative decay rate values, we get $A^{f}_{F_e=5,F_g=4} = A^{nf}_{F_e=5,F_g=4} + A^{coll}_{F_e=5,F_g=4} = 5.24 \times 10^8 \text{ s}^{-1}$.

From the values of $A^{f}_{F_e=5,F_g=4}$, $g_{F_e=5,F_g=4}$, and Eq. (6b), we obtain $\epsilon_{F_e=5,F_g=4} \approx 46$. With this experimental value of the parameter $\epsilon_{F_e=5,F_g=4}$, using approximation (8) we estimate that $\delta V_x^{max} \approx 3.5 \text{ m s}^{-1}$, which is much smaller than $\Delta V_x = 76 \text{ m s}^{-1}$ [which confirms inequality (11)]. Thus the experimental values are compatible with Eqs. (4), (9), (12), and (13) of the simple theoretical model used to explain the origin of the sub-Doppler hyperfine line.

The parametric analysis,[4] based on the model developed by Le Bris *et al.*,[3] of the integrated retrofluorescence spectra at the temperature of 130°C gives the following value for $\epsilon_{F_g=4}$:

$$\epsilon_{F_g=4}\bar{x}^{f}_{eff}\lambda^{-1} = 49, \tag{18}$$

where $\bar{x}^{f}_{eff} \approx \lambda$ is a parameter characterizing the effective geometric depth of the filtering region and λ is the transition wavelength. The parameter $\epsilon_{F_g=4}$ used by the authors in Ref. 4 is an effective coefficient, i.e., it is the same for all the hyperfine levels:

$$\epsilon_{F_e=3,F_g=4} = \epsilon_{F_e=4,F_g=4} = \epsilon_{F_e=5,F_g=4} = \epsilon_{F_g=4}. \tag{19}$$

The value of $\epsilon_{F_g=4}$ evaluated by the parametric method is compatible with our value of $\epsilon_{F_e=5,F_g=4}$ for the cycling $F_e=5\rightarrow F_g=4$ transition line. The qualitative agreement between these two values, taking into account the difference of the two models and the approximations used, confirm the validity of our phenomenological model and experimental method for measuring the atomic Cs$[6^2P_{3/2}(F_e=5)]$ hyperfine level effective nonradiative decay rate $A^{nf}_{F_e=5,F_g=4}$ associated with the interaction between excited atoms and metallic film. The effect of modification of the lifetime of the excited atoms in the vicinity of the metallic film[13,14] is reflected in the spectral properties of the integrated sub-Doppler signal.

The value of the effective nonradiative transfer rate $A^{nf}_{F_e=5,F_g=4} \approx 3.10^8 \text{ s}^{-1}$ seems relatively large compared to the spontaneous emission rate $g_{F_e=5,F_g=4}A_{J_e=3/2,J_g=1/2} \approx 1.14\times 10^7 \text{ s}^{-1}$. The morphology of the metallic film on the cell window at a temperature of 130°C is not known. It can be complex, made of randomly distributed Cs me-

tallic clusters, atoms adsorbed on the clusters, and atoms chemically bonded to the surface. We do not have the necessary information to compare our experimental value of $\epsilon_{F_e=5,F_g=4}$ with a theoretical value that takes into account the real structure of the metallic film. There is no theoretical work, to our knowledge, that has thoroughly analyzed such a case. It is well known that the lifetime of an excited atom in the vicinity of a metallic film is influenced by its nature, thickness, rugosity, complex dielectric constant, and other factors related to the surface effects (surface plasmons) modifying the nonradiative relaxation rate.

5. CONCLUSION

We have confirmed the existence of a sub-Doppler structure in the inhibition spectral band of the retrofluorescence signal, corresponding to the atomic ($6^2S_{1/2} \rightarrow 6^2P_{3/2}$) transition at the interface between glass and saturated Cs vapor at 130°C temperature. Thanks to a comparative analysis with the help of the selective reflection spectroscopy method, we have shown that the sub-Doppler hyperfine structure of this atomic transition coincides with the sub-Doppler structure observed in retrofluorescence. A particular analysis of the hyperfine $[6^2P_{3/2}(F_e=5) \rightarrow 6^2S_{1/2}(F_g=4)]$ transition has been conducted to evaluate the influence of the presence of a metallic film at the interface for this atomic transition. The origin of the sub-Doppler line is mainly governed by the kinematic properties of the populations of the excited velocity classes confined in the vapor layer in the near-field region of the cell. In fact, in this region a fraction of the nonthermalized population of a velocity class behaves like a two-dimensional vapor normal to the laser beam direction, playing the dominant role on the nature of the sub-Doppler profile. The population of a velocity class confined between the metallic film and the far-field region constitutes the effective population of radiating atoms generating the sub-Doppler retrofluorescent signal. The effect of the metallic film on the effective excited atom in the hyperfine $6^2P_{3/2}(F_e=5)$ level in the near-field region has been measured when the cell temperature is 130°C by using simultaneously both the retrofluorescence and FM selective reflection spectroscopic methods. We believe that the utilization of a frequency modulation technique to suppress the retrofluorescent signal originating from the far-field region will improve the observation and the resolution of the sub-Doppler hyperfine signal. Because the cell is slightly tilted, there is an additional broadening mechanism involved. It will be interesting to evaluate the relative value of this effect. Measurements as a function of laser intensity and measurements with the atomic 894 and 455 nm transitions would be interesting to complement the analysis. It is desirable to carry out a more elaborate theoretical development to justify the phenomenological approach used for the estimation of the effective nonradiative relaxation rate of a hyperfine excited level due to the coupling between an excited atomic state and a metallic film. We would also like to point out the physical analogy between the hyperfine spectral properties of our vapor cell and the spectral properties of a vapor confined in an extremely thin cell studied by Sarkisyan *et al.*[15] and Briaudeau *et al.*[11] where the far-field region, in our case, plays the role of a photonic and atomic trap where the population of a velocity class and the resonant photons are thermalized.

ACKNOWLEDGMENTS

We acknowledge financial support for this work from the Natural Sciences and Engineering Research Council of Canada.

REFERENCES

1. K. Zhao, Z. Wu, and H. M. Lai, "Optical determination of alkali metal vapor number density in the vicinity ($\sim 10^{-5}$ cm) of cell surfaces," J. Opt. Soc. Am. B **18**, 1904–1910 (2001).
2. V. G. Bordo, J. Loerke, L. Jozefowski, and H.-G. Rubahn, "Two-photon laser spectroscopy of the gas boundary layer in crossed evanescent and volume waves," Phys. Rev. A **64**, 012903/1–11 (2001).
3. K. Le Bris, J.-M. Gagné, F. Babin, and M.-C. Gagné, "Characterization of the retrofluorescence inhibition at the interface between glass and optically thick Cs vapor," J. Opt. Soc. Am. B **18**, 1701–1710 (2001).
4. J.-M. Gagné, K. Le Bris, and M.-C. Gagné, "Laser energy-pooling processes in an optically thick Cs vapor near a dissipative surface," J. Opt. Soc. Am. B **19**, 2852–2862 (2002).
5. A. M. Akul'shin, V. L. Velichanskii, A. S. Zibrov, V. V. Nikitin, V. V. Sautenkov, E. K. Yurkin, and N. V. Senkov, "Collisional broadening of intra-Doppler resonances of selective reflection on the D_2 line of cesium," Sov. Phys. JETP **36**, 303–307 (1982).
6. V. Vuletic, V. A. Sautenkov, C. Zimmermann, and T. W. Hänsch, "Measurement of cesium resonance line self-broadening and shift with Doppler-free selective reflection spectroscopy," Opt. Commun. **99**, 185–190 (1993).
7. J. Huennekens, R. K. Namiotka, J. Sagle, Z. J. Jabbour, and M. Allegrini, "Thermalization of velocity-selected excited-state populations by resonance exchange collisions and radiation trapping," Phys. Rev. A **51**, 4472–4482 (1995).
8. S. G. Rautian and A. M. Shalagin, *Kinetic Problems of Non-Linear Spectroscopy* (Elsevier Science, 1991).
9. I. I. Sobel'man, *Introduction to the Theory of Atomic Spectra*, Vol. 40 of International Series of Monographs in Natural Philosophy (Pergamon, 1972), p. 297.
10. G. Dutier, S. Saltier, D. Bloch, and M. Ducloy, "Revisiting optical spectroscopy in a thin vapor cell: mixing of reflection and transmission as a Fabry–Perot microcavity effect," J. Opt. Soc. Am. B **20**, 793–800 (2003).
11. S. Briaudeau, D. Bloch, and M. Ducloy, "Sub-Doppler spectroscopy in a thin film of resonant vapor," Phys. Rev. A **59**, 3723–3735 (1999).
12. P. W. Milonni and J. H. Eberly, *Lasers* (Wiley, 1988).
13. C. K. Carniglia, L. Mandel, and K. H. Drexhage, "Absorption and emission of evanescent photons," J. Opt. Soc. Am. **62**, 479–486 (1972).
14. R. R. Chance, A. Prock, and R. Silbey, "Comments on the classical theory of energy transfer," J. Chem. Phys. **62**, 2245–2253 (1975).
15. D. Sarkisyan, T. Becker, A. Papoyan, P. Thoumany, and H. Walther, "Sub-Doppler fluorescence on the atomic D_2 line of a submicron rubidium-vapor layer," Appl. Phys. B **76**, 625–631 (2003).